Journal of Applied Polymer Science

Facile fabrication of double-walled polymeric hollow spheres with independent temperature and pH dual-responsiveness for synergetic drug delivery

Nan Cheng,[1] Yu Wang,[1,2] Feipeng Wu[1]

[1]Technical Institute of Physics and Chemistry, Chinese Academy of Sciences, Beijing 100190, People's Republic of China
[2]University of Chinese Academy of Sciences, Beijing 100049, People's Republic of China
Correspondence to: F. Wu (E-mail: fpwu@mail.ipc.ac.cn)

ABSTRACT: A dual-responsive double-walled polymeric hollow sphere (PHS) serving as a candidate for synergetic drug delivery platform is prepared by a simple and green template polymerization in aqueous medium. The PHS, comprised of thermo-responsive crosslinked poly(*N*-isopropylacrylamide) (PNIPAM) as the inner shell and pH-responsive crosslinked poly(methacrylic acid) (PMAAc) as the outer shell, is assembled through self-removal of the thermo-responsive template from a core-triple shell structure by free radical polymerization with sequential addition of reactants. The discrete double-shell structure renders the PHS independent temperature and pH-controlled swelling/shrinking capability. Taking the advantage of two compartmentalized internal spaces (the core and the interlayer spaces) with independent temperature- and pH-dependent behaviors, two model drugs representing the small molecule and the macromolecule are loaded in selective locations of the PHS. Two drugs show dramatically different release profiles according to environmental temperature and pH, due to the localization of drugs and the stimuli-dependent property of its protective shells.
 J. Appl. Polym. Sci. **2016**, *133*, 44335.

KEYWORDS: biomedical applications; drug delivery systems; phase behavior; swelling

Received 11 March 2016; accepted 5 August 2016
DOI: 10.1002/app.44335

INTRODUCTION

Double-walled polymeric hollow spheres (PHSs) have been increasingly applied in controlling drug release for pharmaceutical application because of the double-layered protection of drug in circulation and enhanced control of drug release.[1–4] It has the potential to overcome the inherent flaws of single-layer hollow spheres such as inability to provide a pulsatile or zero-order release, lack of sustained release specific for periodic therapy and high initial burst. Particularly for temperature and pH dual-responsive double-walled PHSs, it provides further control of drug release to targeting sites and drug release profiles according to environmental stimuli.[5–7] However, the majority effort has been put onto the development of fabrication techniques for well-defined microscale PHS instead of nanoscale.[3,8–12] Specially for nanoscale PHSs, silica-template polymerization is generally applied particularly for dual-responsive double-walled PHSs.[13,14] Typically a functionalized silica core and interlayer is used as a sacrificial template and polymerization proceeds onto the template to establish an alternating silica/polymer multilayer core-triple shell structure, and the corresponding double-walled PHS is obtained after etching the silica core and the interlayer by hydrofluoric acid or sodium hydroxide. Despite successful examples, the synthesis route is time-consuming and possible to bring biotoxicity into the system since organic and corrosive solvents are involved. Therefore, one of the challenges is to develop a simple and green fabrication technique of double-walled PHSs which are feasible to modulate drug release.

Meanwhile, multidrug release in one carrier has been studied in particulate systems, and the release of different therapeutic agents with specific release kinetics in a single carrier has been proved more efficient than a single-drug system.[15,16] Micelles, liposomes, polymeric conjugates and monolayer spheres have been continually reported to use for two or multidrug encapsulation and release.[17–20] For example, a nanoparticle composed of poly(D,L-lactide-*co*-glycolide) (PLGA), Pluronic F127 (PF127), chitosan, hyaluronic acid (HA) and encapsulated with two chemotherapeutic drugs doxorubicin and irinotecan of different anti-tumor mechanisms has been demonstrated up to 500 times enhancement in killing cancer stem-like cells compared to the simple mixture of two drugs.[21] But, the study of co-delivery systems remains inadequate due to the complex

Additional Supporting Information may be found in the online version of this article.

preparation and loading processes, lack of controlled release, the possible drug–drug interactions, and rapid release of hydrophilic agents. Therefore, in our opinion, by virtue of compartmentalized internal space, a double-walled PHS can provide alternative solution for such problems by loading multidrug through selective localization of drugs into specific layers and can be structurally tailored to control release kinetics especially for temperature and pH dual-responsive double-walled PHS. As an example, Shi *et al.* showed a double-walled poly(orthoester)/poly(D,L-lactide-*co*-glycolide) (POE/PLGA) hollow sphere to encapsulate and release two proteins with different water solubility in a more constant manner than a POE or PLGA PHS.[22] However, to fabricate a double-walled PHS particulate system with different compartmental internal space, and process a multidrug loading with controllable release of each drug is still a challenge.

In this article, a simple approach to prepare a dual-responsive double-walled PHS in a single-batch aqueous system is proposed. It is hypothesized that through introduction of a temperature-responsive polymer poly(*N*-isopropylacrylamide) (PNIPAM) instead of silica as the template and to separate two distinctive shells, a core-triple shell microstructure can be easily realized for the corresponding double-walled PHS simply by controlling the addition time of shell monomers and the crosslinker. Based on the choice of shell monomers in this article, the obtained double-walled PHS with temperature-responsive inner shell and pH-responsive outer shell are expected to have two responsiveness existed independently in two separate shells. Furthermore, due to the characteristic two-compartment (the core and the interlayer space) in the PHS, it is attempted for the co-delivery of two model drugs rhodamine B (RhB) and bovine serum albumin-fluorescein isothiocyanate conjugate (FITC-BSA) to explore its potential for synergetic delivery of drugs.

EXPERIMENTAL

Materials

All the reagents were used as received unless otherwise noted. *N*-isopropylacrylamide (NIPAM) was purchased from Aladdin, Shanghai, China. *N,N′*-Methylenebis (acrylamide) (MBA) and ammonium persulfate (APS) were purchased from Lanyi Chemical, Beijing, China. Methacrylic acid (MAAc) was purchased from Xilong Chemical, Guangdong, China. Ultrapure water from a Simplicity® UV water purification system (Merck Millipore, Hong Kong, China) was used for all synthesis reactions, purification, and solution preparation unless otherwise specified.

Synthesize of PNIPAM/PMAAc PHS

The thermo-responsive inner shell was synthesized according to our reported method.[23] Briefly, NIPAM (60 m*M*, 0.339 g) was dissolved in 50 mL water. Right after nitrogen purging for 30 min, APS (0.0065 g in 1 mL water, 1% molar ratio of NIPAM) was added with a syringe, and then increase the temperature of the reaction system to 65 °C. After around 10 min, the crosslinker MBA (0.0091 g in 1 mL water, 2% molar ratio of NIPAM) was injected into the reaction system. The whole reaction was nitrogen protected and was allowed to proceed for 16 h. To isolate the thermo-responsive shell and the following pH-responsive shell, an interlayer of linear PNIPAM (l-PNIPAM) was synthesized and formed outside the thermo-responsive shell. To generate the l-PNIPAM layer, a same amount of NIPAM and APS without MBA was added into the reaction system after the formation of crosslinked PNIPAM shell, and operated according to the procedure for the crosslinked PNIPAM shell. After 12 h reaction to form l-PNIPAM layer, MAAc (54 m*M*, 0.231 mL) and MBA (6 m*M*, 0.04625 g) was predissolved in 50 mL water and added into the reaction system dropwisely after the addition of APS (0.0065 g, 1% molar ratio of MAAc and MBA). The reaction proceeded for 12 h at 65 °C. The resultant solution was allowed to cool down to room temperature, and the pH was adjusted to 8. After stirring for 7 day, the pH of the solution was adjusted to 3, and then the double-walled PHSs were purified and collected by centrifugation at 10,000 rpm for 30 min.

Characterization

Transmission Electron Microscopy (TEM). TEM images were obtained from a transmission electron microscope (JEM-2100, JEOL Ltd., Tokyo, Japan) operating at 200 kV. The samples were prepared onto carbon-coated copper grids, stained with saturated uranyl acetate aqueous solution, and further dried at room temperature under vacuum.

Fourier Transform Infrared Spectroscopy (FTIR) and Nuclear Magnetic Resonance Spectroscopy (NMR). FTIR spectra were determined on an Excalibur HE FTS3100 spectrometer (Digilab, USA) with an attenuated total reflectance (ATR) accessory over a scanning range of 4000–500 cm^{-1}. The ^1H NMR spectrum of PNIPAM/PMAAc PHS was recorded in deuterated dimethyl sulfoxide (DMSO-d6) on an AVANCE III 400MHz Digital NMR Spectrometer (Bruker, Germany).

Dynamic Light Scattering (DLS). 1 mg mL^{-1} PNIPAM/PMAAc PHS aqueous solutions at different pH were first centrifuged at 5000 rpm for 10 min and the supernatants were collected for the DLS experiment. The hydrodynamic radius (R_h) was obtained with a DLS batch (DynaPro® NanoStar®, Wyatt Technology Corp., Santa Barbara, CA, USA) at various temperature points with a 10 min equilibrium time.

Zeta–Potential. 1 mg mL^{-1} PNIPAM/PMAAc PHS aqueous solutions with different pH were prepared by adjusting pH with 1 M HCl and 1 M NaOH solution, and the pH was determined by a pH meter (PHS-25, INESA Scientific Instrument Ltd., Shanghai, China). The zeta-potentials of different samples were obtained from a zetasizer (3000HS, Malvern Instruments Ltd., Malvern, UK).

Lower Critical Solution Temperature (LCST) Determination. The pH of 1 mg mL^{-1} PNIPAM/PMAAc PHS aqueous solutions was adjusted as described above. The LCSTs of PNIPAM/PMAAc PHS aqueous solutions were evaluated by a turbidity method, and the transmittance (%T) was recorded by a UV-Vis spectrophotometer (U-3900, HITACHI, Shanghai, China) at 550 nm. A temperature ramp profile with 2 °C each time and 30 min equilibration for each temperature from 25 to 53 °C was used for samples of pH 6.00, 7.40, and 8.00. The temperature was controlled by a temperature controller (TC-502, Brookfield, Engineering Laboratories, Massachusetts, USA).

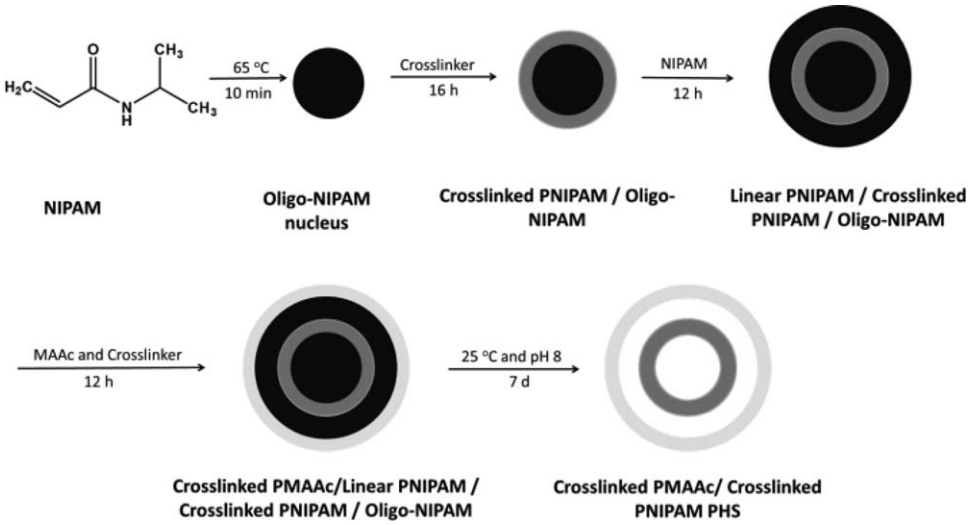

Scheme 1. The synthesis scheme of double-walled PNIPAM/PMAAc PHS.

Drug Loading

RhB loading was performed as below: at 25 °C an approximate 15 mg PNIPAM/PMAAc PHS was dissolved into 5 mL 8 mg mL^{-1} RhB aqueous solution and the pH of the final solution was adjusted to 8.50. The encapsulation proceeded for 2 day with constant agitation. Free and encapsulated RhB were separated by centrifugation (14,000 rpm, 10 min) and the fluorescent intensity of the RhB supernatants before and after encapsulation was measured by fluorescence spectrophotometer (F-4500, HITACHI, Shanghai, China) at the excitation wavelength of 553 nm. The emission spectrum was scanned from 560 to 700 nm with a maximum at 576 nm. The widths of the excitation and the emission slits were 5 and 10 nm respectively. The amount of RhB in the supernatant was quantified from a calibration curve of fluorescent intensity versus concentration of RhB. The encapsulation efficiency (EE%) and loading capacity (LC%) of the PHS were determined by the following equations[24,25]:

$$\text{EE\%} = \frac{\text{total drug} - \text{free drug}}{\text{total drug}} \times 100 \quad (1)$$

$$\text{LC\%} = \frac{\text{total drug} - \text{free drug}}{\text{weight of PHS}} \times 100 \quad (2)$$

FITC-BSA loading was as similar as RhB loading: at 37 °C, an approximately 10 mg RhB preloaded PNIPAM/PMAAc PHS was dissolved into 5 mL 1 mg mL^{-1} FITC-BSA aqueous solution and the pH of the final solution was adjusted to 8.50. The final solution was with constant agitation for 2 day. The fluorescent intensity of the FITC-BSA supernatants before and after encapsulation was measured at the excitation wavelength of 492 nm. The emission spectrum was scanned from 507 to 600 nm with a maximum at 520 nm. The widths of the excitation and the emission slits, as well as the calculation method, were the same as RhB loading study. All the samples were prepared in triplicate.

Drug Controlled Release

RhB and FITC-BSA release profiles were determined by suspending approximately 13 mg of PHS encapsulating RhB and FITC-BSA in 30 mL aqueous solution with different pH and temperature conditions. Four kinds of temperature and pH conditions are as follows: 37 °C and pH 8.50 (Condition 1), 37 °C and pH 3.00 (Condition 2), 25 °C and pH 8.50 (Condition 3), and 25 °C and pH 3.00 (Condition 4), respectively. To maintain the conditions, the sample suspensions were incubated in shaking bathes with 25 and 37 °C at 100 rpm and the pH of the suspensions was preadjusted by 1 M HCl and 1M NaOH.

At appropriate time intervals, 3 mL of each supernatant was taken and a same amount of fresh solvent were added each time to keep the volume of the release medium constant. The amounts of RhB and FITC-BSA were evaluated by measuring fluorescent intensity according to the method mentioned above. The cumulative release percentage was used to allow easy comparison between formulations. It was calculated by summing with the amount at each previous time point and divided by the total amount released.

RESULTS AND DISCUSSION

Preparation of PNIPAM/PMAAc PHS

As illustrated in Scheme 1, the strategy to synthesize the core-triple shell structure and the corresponding double-walled PHS involves three steps: self-template polymerization of crosslinked PNIPAM inner shell, template precipitation polymerization of l-PNIPAM interlayer and pH-responsive PMAAc outer shell, and self-dissolution of the l-PNIPAM core and interlayer.

Specially, in a conventional free radical polymerization initiated by APS in water, a thermo-induced phase transition of oligo-NIPAM appears along with the proceeding of the polymerization, and these oligomer colloids precipitate as the non-crosslinked temperature-responsive cores. Further addition of crosslinking agent MBA into the reaction helps form a crosslinked PNIPAM shell and results in a core-single shell structure of linear oligo-NIPAM core and crosslinked PNIPAM shell. The formation mechanism of the core-shell structure at this stage has been explained in the previous article from our group.[23] Briefly, at temperature above the LCST, oligo-NIPAMs polymerized at the early stage become hydrophobic, stabilized by electrostatic repulsion of the negative change from the aggregate's surface, and thus work as

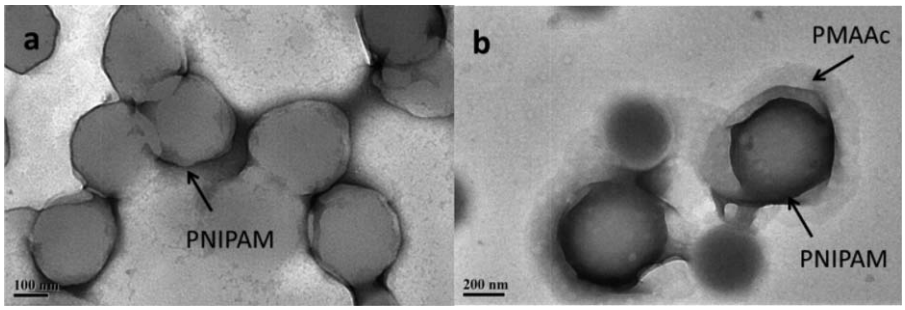

Figure 1. TEM images of (a) the single-walled PNIPAM PHSs and (b) the double-walled PNIPAM/PMAAc PHSs.

templates for the core-shell structure. As the continuous growth of the template, a crosslinker is added to react with oligo-NIPAMs absorbed on the template and form a crosslinked shell around the linear core. Subsequently, to continue the fabrication of multi shells, polymerization of NIPAM without the crosslinker proceeds on the obtained core-single shell structure, linear PNIPAMs absorbed onto the crosslinked shell form an interlayer equivalent to the silica interlayer in silica-template polymerization.[5,13] Continuously, pH-responsive monomer MAAc with MBA is dropwisely added into the system to participate the formation of an outer shell through template precipitation polymerization. Due to the low concentration of MAAc in the reaction system and the formed hydrogen bonds between the template and the monomers, a pH-responsive outer layer formed around the multilayered templates as expected. Finally, the double-walled PHS with distinctive temperature-responsive inner shell and pH-responsive outer shell is obtained after a simple cooling and adjusting pH operation to remove the non-crosslinked core and interlayer.

Overall, the self-template precipitation polymerization with controlled addition of monomers and the crosslinker is applied to prepare a double-shell hollow nanoparticle in aqueous medium. During the polymerization, the growing polymer chains precipitate onto the hydrophobic oligo-NIPAM aggregate to form a polymer shell and further react with absorbed crosslinker MBA to form a crosslinked shell. The following layers of l-PNIPAM and crosslinked PMAAc are all in accord with the same theory. Meanwhile, it is believed that the formation of hydrogen bonds between acidic units and amide segments helps increase the localized concentration of MAAc on the surface of the spheres, promotes the polymerization, and therefore avoids the formation of free microgels. As a result, a core-triple shell structure is obtained in a single pot, and a double-walled hollow structure forms *via* simple tuning of temperature and pH of the system. Decrease of temperature below the LCST turns NIPAM segments to hydrophilic and enlarges the pore in PNIPAM shell, while increase of pH to 8 enlarges the pore in PMAAc shell. The swelling of both shells facilitates penetration of dissolved template through the crosslinked shells and results in a hollow structure with two compartments. Finally, decreasing the pH again, the outer shells become hydrophobic and aggregate to form colloids, and this helps separate the dissolved non-crosslinked PNIPAM and the colloidal PHSs by centrifuge.

Reviewing the fabrication conditions, it can conclude that the polymerization is conducted in the aqueous solution without organic solvents; the reaction is controlled at mild temperature (65 °C); most importantly, the assembly of the core-triple shell structure is completed in a single pot. These improvements in fabrication including a simplified synthesis and avoidance of toxic solvents (compared with traditional silica-template polymerization) will be definitely favorable for its further applications to encapsulate drugs or other bioactive molecules.

Characterization of PNIPAM/PMAAc PHS

TEM provides direct evidence on successful fabrication of double-walled hollow structure. As is revealed in Figure 1, a typical hollow nanosphere structure with a light contrast of the inner cavity and a deep contrast of the shell is seen in both images. The light core regions in both images correspond to the hollow interior left after the self-removal of the linear template and suggest that the linear template has been successfully removed by dissolution and diffusion into the medium below LCST. The full circle structure is visible in both single- and double-walled PHSs, as evidence on the successful template precipitation polymerization to form continuous shells. Furthermore, as shown in Figure 1(b), the shells present with contrast variation and the light-contrast shell is dispersed in a loose net-like state in comparison with the deep-contrast inner shell in an aggregate state. These indicates the existence of two shells with distinct chemical composition and further imply that the crosslinked PMAAc shell has been successfully encapsulated onto the PNIPAM PHS as described in Scheme 1. It is believed that the different contrast is likely due to the different degree of interaction between PNIPAM or PMAAc and the dye uranyl acetate. The dents in the PHSs demonstrate the PNIPAM inner shell and the PMAAc outer shell keep flexible. To further confirm the existence of PMAAc layer, both ATR-FTIR and ^{1}H NMR spectroscopy were conducted. In the IR spectra (Supporting Information Figure S1), the characteristic bands at 1532, 1640, and 3285 cm^{-1} in both single- and double-walled PHSs are associated with the vibration of the PNIPAM layer. The existence of characteristic band of COOH group at 1710 cm^{-1} is observed for PNIPAM/PMAAc PHS and is further evidence to the existence of PMAAc layer. In ^{1}H NMR spectrum (Figure 2), the characteristic chemical shifts of carboxylic acid, amide and isopropyl groups at 12.36 ppm, 7.23 ppm and 3.86 ppm are all observed, and prove the existence of NIPAM and MAAc. As far, the resultant PHS has been confirmed by several methods as a double-walled microstructure with distinct chemical composition in two walls.

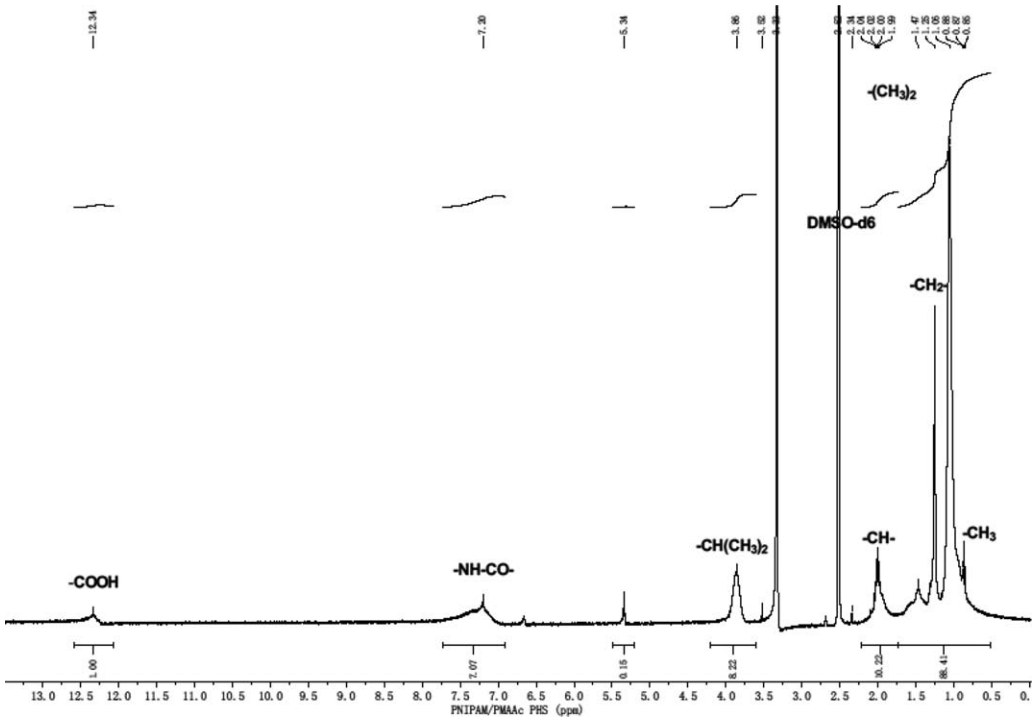

Figure 2. The ^{1}H NMR spectrum of PNIPAM/PMAAc PHS.

The composition of the PHS is determined by ^{1}H NMR. The molar fractions of PMAAc, PNIPAM, and MBA in PNIPAM/PMAAc PHS are calculated according to the integral of the methenyl proton from NIPAM at 3.86 ppm, the methenyl proton from the back bone of NIPAM and MBA at 2.02 ppm, and the peaks between 0.50 and 1.70 ppm corresponding to the methylene protons in the two shells with the methyl protons from both PNIPAM and PMAAc. The result shows that the PHS is composed of 63% NIPAM unit, 29% MAAc unit and 8% MBA unit. The molar ratio between thermo-responsive NIPAM and pH-responsive MAAc is 2.2. This high content of PMAAc in PNIPAM/PMAAc is considered as another advantage of our strategy to increase the applicable percentage of hydrophilic MAAc in a dual-responsive polymeric architecture.

Temperature and pH-Responsive Behaviors of PNIPAM/PMAAc PHS

To elaborate the responsive characteristics of the double-walled microstructure and its independence, the thermo- and pH-responsive behaviors were investigated separately with different methodologies.

The pH-responsiveness is first demonstrated by the transparency change of PNIPAM/PMAAc PHS aqueous solutions at different pH (determined by the pH meter and applied for all the following experiments) at room temperature (Figure 3). At pH 2 and 3 the carboxylic acid groups remain a nonionized state and the hydrophobic nature of PMAAc is dominant, which lead to the shrinking of the PMAAc shell due to hydrophobic interaction. Meanwhile, the motion of the inner PNIPAM segments is restricted due to the increased hydrogen bonding between amide in PNIPAM and carboxylic acid group in PMAAc, as well as the limited space. The restricted inner shell and the uncharged outer shell intend to break the stability of the colloids and form large aggregates with each other. As a result, sedimentation is observed. When the pH increases to 4 and 5, the carboxylic acid groups are partially deprotonized and the hydrophobic effect of the PMAAc shell gets weakened. This causes the swelling of the outer layer, frees the inner PNIPAM shell due to interruption of hydrogen bonds, and moreover helps stabilize the aggregates of the PHSs all through weak electrostatic repulsion among the partially negative-charged outer shells. But it is believed that the inner PNIPAM segments are still in a restricted state and maintain as loose aggregates. Therefore, a uniform suspension with a low transparency appears. At pH 6 and above, where the carboxylic acid groups are fully deprotonized, the hydrophilic effect of PMAAc increases along with the increased pH, and more hydrogen bonds are interrupted resulting in more free PNIPAM segments. These leads to the formation of relative small aggregates or no aggregates due to the enhanced electrostatic repulsion and contributes to an increased transparency,[26] as shown in the image.

To understand the influence of both pH and temperature on the swelling behaviors of PNIPAM/PMAAc PHS in depth, the dynamic light scattering (DLS) technique was brought in to investigate pH and temperature-dependent size change of the PHS. First, hydrodynamic radii (R_h) of samples in aqueous media of 25 °C at a constant pH from 4.1 to 9 were studied. The expected pH and temperature-induced volume phase transition (VPT) behavior is shown in Figure 4. As seen in Figure 4(a), the R_h of PNIPAM/PMAAc PHS increases from 156 to 369 nm when the pH value of the solution is from 4.1 to 9, and the diameter reaches the maximum when the value is 6 and

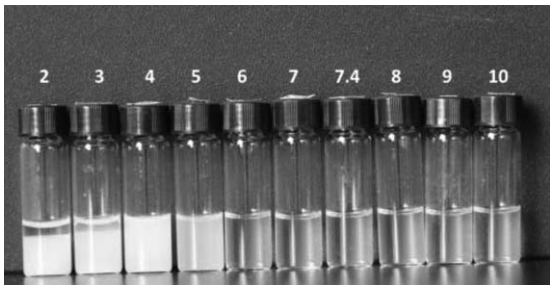

Figure 3. Photographs of PNIPAM/PMAAc PHS aqueous solutions (2 mg·mL^{-1}) with pH from 2 to 10 (from left to right, as labeled on top of vials) at 25 °C.

above. The swelling ratio (defined as the ratio of swollen to deswollen capsule radius) of PNIPAM/PMAAc PHS is 2.4. As known, the crosslinking degree, which is 10 mol% in the PMAAc shell of PNIPAM/PMAAc PHS, has a crucial impact on R_h and is usually kept in a lower level in the formation of crosslinked polymeric shell. But thanks to the structure we can use a relative high crosslinking degree and still maintain a reasonable swelling ratio, which is comparable with multilayer polyelectrolytes capsules.[27] Most importantly, unlike hydrophilic pH-responsive units in a copolymer of thermo-responsive and pH-responsive units, which need to be controlled in a very low percentage (below 10%) to maintain dual-responsiveness in a practicable range,[28,29] PNIPAM/PMAAc PHS keeps a relative low molar ratio between thermo-responsive PNIPAM and pH-responsive PMAAc. Therefore, for MAAc in a copolymer of P(NIPAM-co-MAAc), the molar ratio of MAAc usually kept in a very low level and, in some cases, incorporated with a positive charged hydrophobic compounds to lower the LCST to a reasonable range at a specific pH.[30–32] But for the double-walled PHS prepared in this strategy, the characteristic double-walled structure keeps thermo- and pH-sensitivity independently in each layers of the PHS. This independence is believed as one of the solutions to avoid compromise of thermo-sensitivity when hydrophilic pH-sensitive unit is introduced, and one alternative to keep a high ratio of MAAc in a temperature and pH dual-responsive PNIPAM/PMAAc microstructure. As is discussed above, this pH-dependence change of the size is clearly a consequence of the fact that the carboxylic acid groups in the crosslinked PMAAc shell are deprotonized at high pH values, become more hydrophilic and the swelling of the shell is thus triggered owing to electrostatic repulsion and osmotic pressure to reach Donnan equilibrium.[13] At pH conditions from 4.1 to 6, some of the carboxylic acid groups are ionized and the electrostatic repulsion between the negative-charged groups results in an enhanced swelling. Moreover, the ionization also causes an increase in ion osmotic pressure which is favor to the swelling. When the pH reaches around 6 and above, all carboxylic groups turn into the ionized form and then the maximum swelling is obtained. This result is consistent with the naked eye observation of the PNIPAM/PMAAc PHS aqueous solution at different pH in Figure 3. To clearly illustrate the change of the void space over pH and the drug loading capacity, a calculation was conducted to show the volume change according to pH. As shown in Figure 4(b), at 25 °C the PHS expands about 13.2 times in volume from pH 4.1 to 9. The excellent expanding capacity and the obtained large cavity could be recognized extraordinary as a drug carrier to load a large amount of drugs and release them efficiently according to pH change, and maintain a lower material/drug ratio as well.[33,34] Additionally, the change in diameter over pH provides more evidence on the presence of the PMAAc layer. The swelling ratio according to pH is comparable with previous reported single-shell PMAAc PHS by silica-template polymerization[35] and indirectly demonstrates the independence of the PMAAc shell.

Since the thermo-responsive shell is encapsulated in the pH-responsive one, its thermo-induced change is relatively hard to be investigated. Fortunately, the thermo-induced aggregation of the PNIPAM shell was captured by DLS. First, a constant increase of the size distribution around 45–84 nm in comparison with the constant decrease of that around 389–489 nm in response to the increased temperature (from 25 to 37 °C) is observed and it indirectly indicates the thermo-induced shrinking of the inner shell (Supporting Information Figure S2). Meanwhile, as is presented in Figure 4(a), due to a restricted PMAAc outer shell, the change of the size for PNIPAM/PMAA PHS could be neglected while the temperature is increased from 25 to 37 °C. However, the shrinking of temperature-responsive PNIPAM inner shell induced by the increased temperature can be observed by the appearance of a new size distribution around 63 nm. Although it does not represent the real R_h of the inner shell (since the swollen outer shell has different optical property compared to the aqueous medium even though it contains a large amount of water, and the collected scattered light from the inner shell surface and the frequency do not fit the algorithm), the appearance of this new distribution at the temperature above LCST is still a sign of the thermo-induced aggregation of the PNIPAM inner shell. Both Supporting Information Figures S2 and 4(a) strongly support the conclusion that the enhanced hydrophobic interaction of PNIPAM is induced by the increased temperature and the shrinking of the inner shell results in a more compact inner aggregate, which could be captured by the laser. Additionally, it implies that the two shells are independent, and can independently response to temperature and pH. A turbidity experiment of PNIPAM/PMAAc PHS aqueous solution at different pH was also conducted to corroborate this conclusion (Supporting Information Figure S3).

These structural and responsiveness results suggest that, for drug delivery application, the guest molecules encapsulated in the cavity need to pass through two layers of protection which are controlled independently by temperature and pH, and only when both environmental temperature and pH satisfy the swelling characteristic of two independent shells the guest molecules could be released. In contrast, the guest molecules which are encapsulated in the interlayer area just require passing through the protection of a single pH-responsive outer shell. This specific localization of drugs in PNIPAM/PMAAc PHS could provide different release profiles of drugs according to environmental temperature and pH, which opens the opportunity to be used as a vector to deliver synergetic drugs with different therapeutic mechanisms and required sequential release.

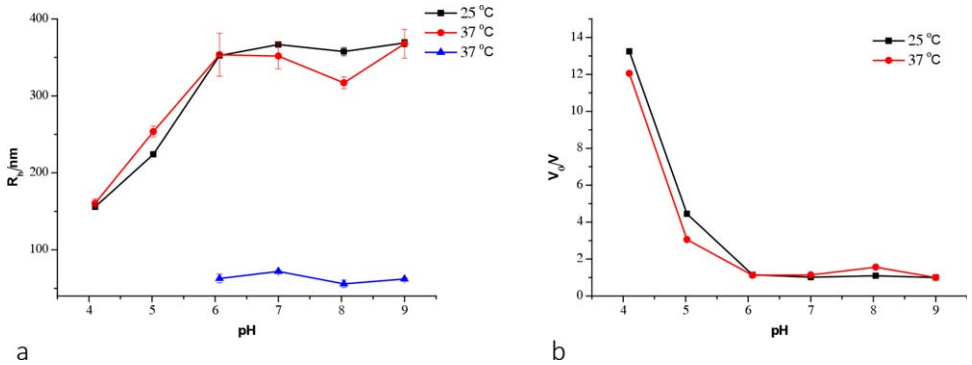

Figure 4. (a) The hydrodynamic radii (R_h) of PNIPAM/PMAAc PHSs in aqueous media vs pH from 4.1 to 9 at 25 °C and 37 °C, respectively. Note: Two size distributions appear for PNIPAM/PMAAc PHS aqueous solution at 37 °C and, therefore, two corresponding R_h profiles (Red dot and blue triangle) are shown; (b) calculated volume changes of PNIPAM/PMAAc PHSs from pH 4.1–9 by assuming the volume at pH 9 as V_0. [Color figure can be viewed at wileyonlinelibrary.com.]

Encapsulation and Release of RhB and FITC-BSA

Several groups have investigated and proved double-layered spheres as drug depots for either pulse release or long time zero-order release.[24,36] The applicable purpose of our design is to provide a vector to manipulate release of two synergetic drugs and aim to control the release profiles by environmental temperature and pH. Therefore, followed by the aforementioned loading processes, the drug release profile of fluorescent RhB and FITC-BSA from PNIPAM/PMAAc PHS at different temperature and pH was studied. First, through the control of the swelling status of both shells, two drugs could be loaded into different void spaces of the PHS: RhB in the core area and FITC-BSA in the interlayer space. According to the calculation methods mentioned [eqs. (1) and (2)] in the experimental section and the initial concentrations used for both drugs, the EE % and the LC % of RhB are 76.3 ± 5.8% and 29.2 ± 2.2% respectively while they are 9.3 ± 2.9% and 4.3 ± 1.3% for FITC-BSA.

The releases were shown in Figure 5. It is observed that both the medium temperature and the pH have significant effect on the drug release. The release of preloaded drugs is manipulated by the swelling/shrinking state of shells induced by environmental temperature and pH. As seen in the release profile of RhB under four conditions in Figure 5(a), at Condition 3, the release of RhB is significantly increased compared to the other three conditions, which demonstrates that the release is triggered by simultaneous temperature and pH. It is clear that when the inner and outer shells swell RhB loaded in the core can be easily

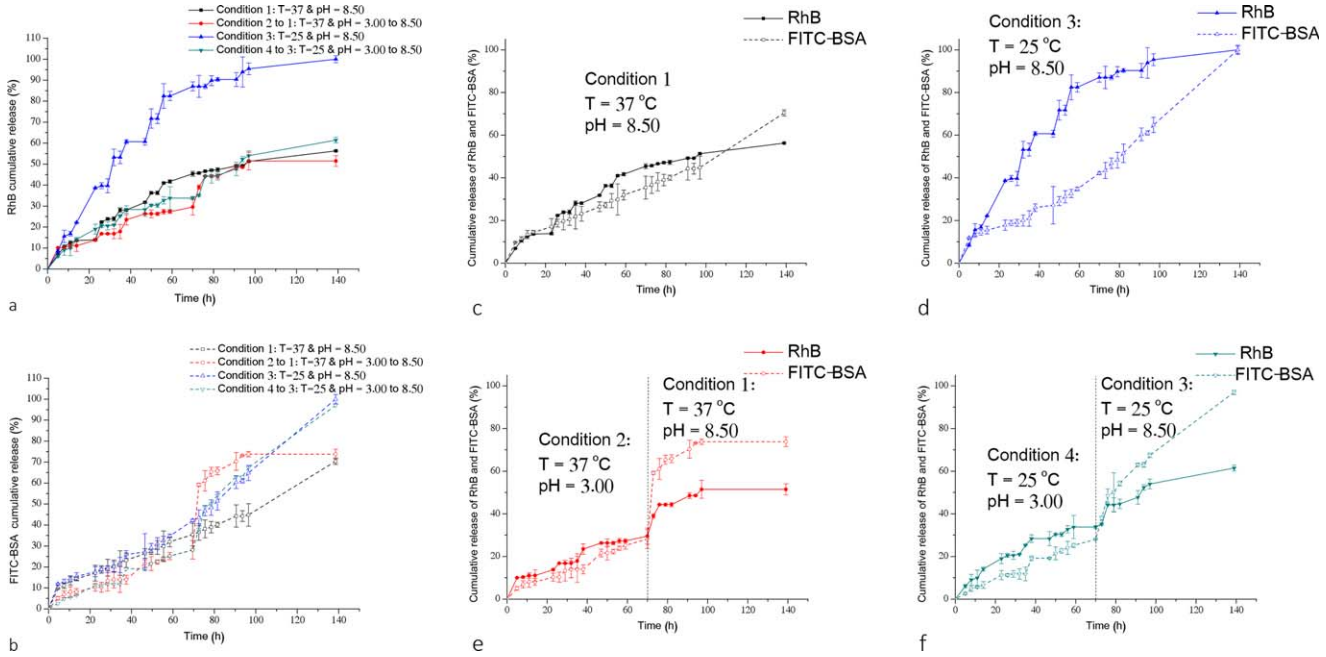

Figure 5. (a) Cumulative release (%) of RhB at four different environmental conditions; (b) cumulative release (%) of FITC-BSA at four different environmental conditions; cumulative release of RhB and FITC-BSA at (c) Condition 1: 37 °C and pH 8.50, (d) Condition 3: 25 °C and pH 8.50, (e) Condition 2 to 1: 37 °C and pH 3.00 to 8.50 at 70 h and (f) Condition 4 to 3: 25 °C and pH 3.00 to 8.50 at 70 h. [Color figure can be viewed at wileyonlinelibrary.com.]

Table I. The Diffusional Exponent (n) and Correlation Coefficient (R^2) Obtained from the Power Law Equation Fitting of Experimental Data

	Medium condition	n	R^2
For RhB	Condition 1: 37 °C and pH 8.50	0.66	0.97
	Condition 2: 37 °C and pH 3.00	0.49	0.89
	Condition 3: 25 °C and pH 8.50	0.76	0.96
	Condition 4: 25 °C and pH 3.00	0.64	0.98
For FITC-BSA	Condition 1: 37 °C and pH 8.50	0.55	0.96
	Condition 2: 37 °C and pH 3.00	0.70	0.84
	Condition 3: 25 °C and pH 8.50	0.61	0.87
	Condition 4: 25 °C and pH 3.00	0.86	0.97

released through two swollen layers, not at the other three combinations of temperature and pH where either the inner or the outer shell maintains a shrunken state to prevent diffusion of RhB. Therefore, the swollen status of two independent shells determines the RhB release profile collaboratively. Furthermore, when switch environmental pH from 3.00 to 8.50 at 70 h, a burst release is observed in both samples at 37 and 25 °C in Figure 5(a). Meanwhile, the total cumulative releases for the two samples with varied pH reach 51.5% for the sample at 37 °C and 61.5% for the one at 25 °C, which are comparative to the total cumulative release of the sample at 37 °C and pH 8.50 (Condition 1). The result implies that dense either the outer shell or the inner shell retards the diffusion of RhB from the core to the environment. In contrast, for FITC-BSA, due to the specific loading location the release is only regulated by pH and the temperature has little impact on the release of FITC-BSA [Figure 5(b)]. Before 70 h the release at four different conditions generally follows two kinds of profiles according to the pH conditions. After 70 h, since the change of pH to 8.50 for the two samples initially at 3.00, a pulse release is observed and the total cumulative releases of these two samples are equivalent to those initially at pH 8.50. It indicates that pH plays a crucial role on FITC-BSA release.

To further elucidate the release difference between RhB and FITC-BSA at a same environmental condition, release profiles of both drugs at the same temperature and pH condition were plotted and analysed. By comparing the release of RhB and FITC-BSA at a same condition, it clearly demonstrates the delivery of two drugs in one carrier can be independently manipulated through the swollen status of two separate shells of PNIPAM/PMAAc PHS. At Condition 1 [Figure 5(c)], both drugs are gradually released, but the release of FITC-BSA is slightly faster than RhB; at Condition 3 [Figure 5(d)] the release of RhB is significantly faster than FITC-BSA. It is obvious that the burst release of RhB at Condition 3 is a result of RhB fast diffused out of swollen inner and outer shells. Surprisingly, comparing the FITC-BSA cumulative release in Figure 5(c,d), when the temperature changes from 37 to 25 °C the cumulative release of FITC-BSA is slightly affected even at the same pH condition (pH 8.50) where the outer shell maintains swollen state. It increases 29.6% from Condition 1 to Condition 3. It is believed that the variation is caused by the hydrophobic nature of the inner PNIPAM shell at 37 °C resulting in an increased affinity to FITC-BSA, preventing its diffusion.[37,38] At Condition 2, both shells maintain a shrunken state and there is no considerably difference between release profiles of RhB and FITC-BSA. As seen in Figure 5(e), the releases follow the same trend of low release rate before 70 h and reached about 29.5% of the total cumulative release for RhB and 28.2% for FITC-BSA at 70 h right before the change of pH condition. The low release of both drugs at Condition 2 is likely due to osmotic pressure, thus causing the leaching of drugs into the medium. Whereas at Condition 4 the swollen inner shell increases the release of RhB but the release is delayed by the shrunken and compact outer shell due to a longer mass transport pathway. Therefore the release of RhB at this condition is just 35.4% while the release of FITC-BSA remained 28.0% at 70 h [Figure 5(f)], affirming that the compact PMAAc layer at a low pH serves as a rate-limiting barrier against both drug releases. Therefore, this confirmative stimuli-dependent drug release and the two-compartment structure are of particular interest for drug storage in synergetic drug delivery. As expected, it can control multi-drug release with independent mechanism. It is also expected that PNIPAM/PMAAc PHS with its specific structure and independent responsive properties can minimize drug–drug interaction, and improve the drugs' performance by the sequential release of drugs in specific sites.

To evaluate the release kinetics, the semi-empirical power law equations introduced by Siepmann and Peppas[39] was attempted to analyze the release behavior. The values of diffusional exponent (n), correlation coefficient (R^2) and release rate coefficients (k) obtained from this modified Peppas equation[24] are summarized in Table I. It is shown that the n values for the release of RhB and FITC-BSA at four conditions are between 0.43 and 0.85, suggesting anomalous release behavior. In the case of RhB, at Condition 1 the log cumulative releasing amount *vs* time yields good linearity ($R^2 = 0.97$) with an exponential n at 0.66. It indicates at this condition the release of RhB from PNIPAM/PMAAc PHS follows the combination mechanism of Fickian diffusion (Brownian motion) and Case II transport (polymer relaxation), which is likely due to the different state of two shells: the inner one is shrunken and the outer one is swollen. At Condition 2, the n value is 0.49 and the R^2 is 0.89. Under this high temperature and low pH environment, hydrophobic interaction and hydrogen bonding among PNIPAM and PMAAc chains have been strengthened and thus the movement of polymer chains is limited due to enhanced

polymer–polymer interaction. Therefore, it is believed that the transport of RhB here is mainly attributed to Brownian motion (e.g., Fickian diffusion) in the collapsed PHS, which results in a relative low n value. When the environment is at Condition 3, the swelling of both shells accelerates the transport of RhB and obviously polymer relaxation plays a dominant role in the transport and, as a result, a higher n value ($n = 0.76$) is obtained from the estimation with a relatively good coefficient of correlation ($R^2 = 0.96$). At Condition 4, the outer shell keeps a shrunken state but the inner shell is swollen. The n value is 0.64 and the R^2 is 0.98. Its n value is comparable to that at Condition 1, where the two shells are in a reverse state. It is resulted from the superposition of both effects, playing equivalent roles on the release kinetics.

Different from RhB release, in the case of FITC-BSA protected only by pH-sensitive PMAAc layer as seen in Table I, the n values can be divided into two groups: 0.55 for Condition 1 and 0.61 for Condition 3; 0.70 for Condition 2 and 0.86 for Condition 4. It is obvious that pH is a decisive factor on the release kinetics regardless of temperature for FITC-BSA. All four releases are still under an anomalous transport mechanism, and diffusion has a more important impact over polymer relaxation at low pH since the hydrophobic interaction at low pH is enhanced.

Overall, a new single-batch strategy to prepare PHS is demonstrated, and a double-walled PHS with independent thermo- and pH-responsiveness has been successfully fabricated in a complete aqueous system. The microstructure has been confirmed by TEM and the responsive properties towards temperature and pH have been studied through the variation of the hydrodynamic radius. The release of RhB and FITC-BSA selectively encapsulated in specific locations of the PHS follows different profiles under varied temperature and pH conditions, and burst release of both drugs can be observed through manipulation of temperature or pH.

CONCLUSIONS

In summary, a simple, green and versatile self-removable template polymerization to create double-walled PHS with independent thermo- and pH-responsiveness has been demonstrated. Through the utility of thermo-induced aggregation of PNIPAM, fabrication of double-walled structure can be achieved in a single-batch aqueous reaction system with mild conditions, and the use of organic and corrosive solvents is avoided. A strong dependence of drug release over pH and temperature has been observed and can be explained by the independent swelling/shrinking behaviors of both shells of the PHS. According to the procedure, the cavity, the void between the two shells and the thickness of the shells may be easily adjusted by the feeding time of reactants and the initial monomer concentration, and the choice of monomers is definitely broadened by just using conventional free radical polymerization. Hence, we believe this strategy holds great promise for large-scale production of series of such double-walled PHSs with potential in controllable delivery of synergetic drugs.

REFERENCES

1. Yin, D. Z.; Li, B. Q.; Liu, J. J.; Zhang, Q. Y. *Colloid Polym. Sci.* **2015**, *293*, 341.
2. Xia, Y.; Ribeiro, P. F.; Pack, D. W. *J. Controlled Release* **2013**, *172*, 707.
3. Berkland, C.; Cox, A.; Kim, K.; Pack, D. W. *J. Biomed. Mat. Res. A* **2004**, *70A*, 576.
4. Lee, T. H.; Wang, J. J.; Wang, C. H. *J. Controlled Release* **2002**, *83*, 437.
5. Du, P.; Wang, T.; Liu, P. *Colloids Surf. B* **2013**, *102*, 1.
6. Chiang, W. H.; Viet Thang, H.; Huang, W. C.; Huang, Y. F.; Chern, C. S.; Chiu, H. C. *Langmuir* **2012**, *28*, 15056.
7. Qian, J.; Wu, F. *J. Mat. Chem. B* **2013**, *1*, 3464.
8. Shchukina, E. M.; Shchukin, D. G. *Curr. Opin. Colloid Interface Sci.* **2012**, *17*, 281.
9. Rossier-Miranda, F. J.; Schroen, K.; Boom, R. *Food Hydrocolloids* **2012**, *27*, 119.
10. Xia, Y. J.; Xu, Q. X.; Wang, C. H.; Pack, D. W. *J. Pharm. Sci.* **2013**, *102*, 1601.
11. De Cock, L. J.; De Koker, S.; De Geest, B. G.; Grooten, J.; Vervaet, C.; Remon, J. P.; Sukhorukov, G. B.; Antipina, M. N. *Angew. Chem. Int. Ed.* **2010**, *49*, 6954.
12. Quinn, A.; Such, G. K.; Quinn, J. F.; Caruso, F. *Adv. Funct. Mater.* **2008**, *18*, 17.
13. Li, G.; Lei, C.; Wang, C. H.; Neoh, K. G.; Kang, E. T.; Yang, X. *Macromolecules* **2008**, *41*, 9487.
14. Xing, Z.; Wang, C.; Yan, J.; Zhang, L.; Li, L.; Zha, L. *Colloid Polym. Sci.* **2010**, *288*, 1723.
15. Meng, H.; Liong, M.; Xia, T.; Li, Z.; Ji, Z.; Zink, J. I.; Nel, A. E. *ACS Nano* **2010**, *4*, 4539.
16. Wu, J.; Lu, Y.; Lee, A.; Pan, X.; Yang, X.; Zhao, X.; Lee, R. *J. J. Pharm. Pharm. Sci.* **2007**, *10*, 350.
17. Singh, A.; Dinawaz, F.; Mewar, S.; Sharma, U.; Jagannathan, N. R.; Sahoo, S. K. *ACS Appl. Mater. Interfaces* **2011**, *3*, 842.
18. Xiong, X. B.; Lavasanifar, A. *ACS Nano* **2011**, *5*, 5202.
19. Aryal, S.; Hu, C. M. J.; Zhang, L. F. *Small* **2010**, *6*, 1442.
20. Wang, H. J.; Zhao, P. Q.; Su, W. Y.; Wang, S.; Liao, Z. Y.; Niu, R. F.; Chang, J. *Biomaterials* **2010**, *31*, 8741.
21. Wang, H.; Agarwal, P.; Zhao, S.; Xu, R. X.; Yu, J.; Lu, X.; He, X. *Biomaterials* **2015**, *72*, 74.
22. Shi, M.; Yang, Y. Y.; Chaw, C. S.; Goh, S. H.; Moochhala, S. M.; Ng, S.; Heller, J. *J. Controlled Release* **2003**, *89*, 167.
23. Qian, J.; Wu, F. *Chem. Mater.* **2007**, *19*, 5839.
24. Pinheiro, A. C.; Bourbon, A. I.; Cerqueira, M. A.; Maricato, É.; Nunes, C.; Coimbra, M. A.; Vicente, A. A. *Carbohydr. Polym.* **2015**, *115*, 1.
25. Shu, S.; Sun, C.; Zhang, X.; Wu, Z.; Wang, Z.; Li, C. *Acta Biomater.* **2010**, *6*, 210.
26. Pich, A.; Tessier, A.; Boyko, V.; Lu, Y.; Adler, H. J. P. *Macromolecules* **2006**, *39*, 7701.
27. Constantin, M.; Bucatariu, S.; Harabagiu, V.; Popescu, I.; Ascenzi, P.; Fundueanu, G. *Eur. J. Pharm. Sci.* **2014**, *62*, 86.

28. Fundueanu, G.; Constantin, M.; Asmarandei, I.; Harabagiu, V.; Ascenzi, P.; Simionescu, B. C. *J. Biomed. Mater. Res. A* **2013**, *101*, 1661.
29. Kleinen, J.; Klee, A.; Richtering, W. *Langmuir* **2010**, *26*, 11258.
30. Zhou, W. T.; An, X. Q.; Gong, J.; Shen, W. G.; Chen, Z. Y.; Wang, X. Y. *J. Appl. Polym. Sci.* **2011**, *121*, 2089.
31. Kleinen, J.; Richtering, W. *J. Phys. Chem. B* **2011**, *115*, 3804.
32. Wong, J. E.; Díez-Pascual, A. M.; Richtering, W. *Macromolecules* **2009**, *42*, 1229.
33. Chen, Y.; Chen, H. R.; Zeng, D. P.; Tian, Y. B.; Chen, F.; Feng, J. W.; Shi, J. L. *ACS Nano* **2010**, *4*, 6001.
34. Chen, L. B.; Zhang, F.; Wang, C. C. *Small* **2009**, *5*, 621.
35. Li, G.; Shi, Q.; Yuan, S. J.; Neoh, K. G.; Kang, E. T.; Yang, X. *Chem. Mater.* **2010**, *22*, 1309.
36. Lee, W. L.; Guo, W. M.; Ho, V. H. B.; Saha, A.; Chong, H. C.; Tan, N. S.; Tan, E. Y.; Loo, S. C. J. *Acta Biomater.* **2015**, *27*, 53.
37. Shamim, N.; Hong, L.; Hidajat, K.; Uddin, M. S. *J. Colloid Interface Sci.* **2006**, *304*, 1.
38. Ding, X. B.; Sun, Z. H.; Zhang, W. C.; Peng, Y. X.; Wan, G. X.; Jiang, Y. Y. *J. Appl. Polym. Sci.* **2000**, *77*, 2915.
39. Siepmann, J.; Peppas, N. A. *Adv. Drug Deliv. Rev.* **2001**, *48*, 139.